# Modelling the formation of the galactic bulge

O. Cavichia[1] & M. Mollá[2]

[1] Instituto de Física e Química, Universidade Federal de Itajubá, Av. BPS, 1303, 37500-903, Itajubá-MG, Brazil e-mail: `cavichia@unifei.edu.br`

[2] Departamento de Investigación Básica, CIEMAT, Avda. Complutense 40, E-28040 Madrid, Spain e-mail: `mercedes.molla@ciemat.es`

**Abstract.** In this work we have assumed a Hernquist model with an inside-out formation for the Galactic bulge and, using a chemical evolution model, we were able obtain the bulge metallicity distribution function (MDF) for different radial regions. The preliminary results show that in the inner regions of the bulge the MDF has a higher fraction of metal poor stars, while this fraction is progressively diminished as moving outwards in the bulge. These results may explain the metallicity gradient observed in the Galactic bulge.

**Resumo.** Neste trabalho assumimos um modelo de Hernquist com uma formação interna-externa para o bojo Galáctico e, usando um modelo de evolução química, fomos capazes de obter a distribuição de metalicidades do bojo (MDF) para diferentes regiões radiais. Os resultados preliminares mostram que nas regiões internas do bojo a MDF apresenta uma fração maior de estrelas pobres em metais, enquanto que esta fração diminui movendo-se para as regiões externas do bojo. Estes resultados podem explicar o gradiente de metalicidades observado no bojo Galáctico.
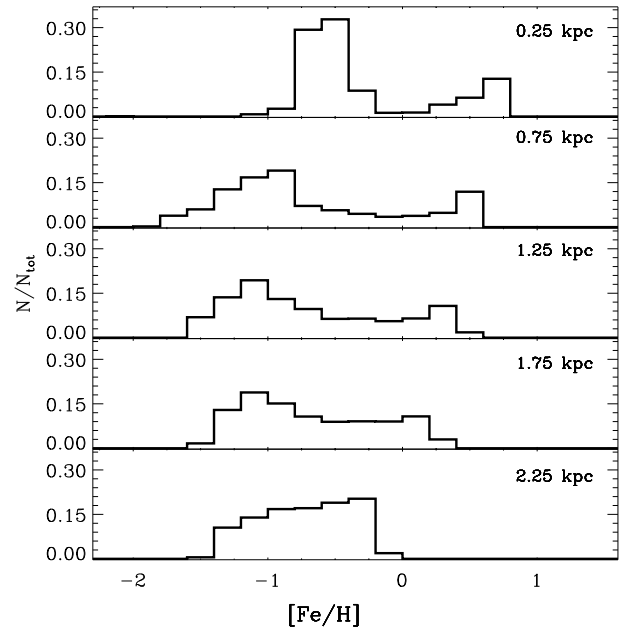
**Keywords.** Galaxy: bulge – Galaxy: evolution – Galaxy: formation

## 1. Introduction

The Galactic bulge (GB) is the only galaxy bulge that can be resolved and can be studied with exquisite details. Hence, the bulge metallicity distribution function (MDF) can be traced for different regions within the bulge and can give us clues about the bulge formation scenario. Recently, observations (e.g. Zoccali et al. 2008, Rojas-Arriagada et al. 2014) have shown that the GB is composed of at least two components with different mean metallicities, and possibly different spatial distribution and kinematics. Zoccali et al. (2017) have demonstrated that the two components present a different spatial distribution, with the metal poor population being more centrally concentrated. There is no consensus in the literature regarding if this result point to a GB formation scenario formed by a bar instability or if the the GB formed from a spheroidal collapse. In this regarding, chemical evolution models (CEM) are important tools to understand the formation and evolution of the components of the Milky Way Galaxy (MWG) and other galaxies in the universe. The outputs generated by the CEM are compared with the observational data and the physics adopted is changed self-consistently until satisfactory results are achieved. Precisely, one of the most important constraints for CEM is the metallicity distribution function (MDF). In particular, the MDF of a region is sensible to the timescale that the region was formed.



**Figure 1.** Fe/H] histograms for different regions in the GB (0.25, 0.75, 1.25, 1.75 and 2.25 kpc), as labeled in each panel. The theoretical MDFs represent those from giant GB stars, being the stellar abundances computed taking into account the stellar life-times from Padova isochrones.

## 2. Model and results

Our model is an update of the one from Mollá & Díaz (2005) and the GB is formed assuming an inside-out growth scenario where the accretion of metal-poor gas from the halo builds the spheroidal component and also the disc. The infall rate for each radial region is given in Mollá et al. (2016) and is obtained by imposing that after a Hubble time the system ends with a mass as observed for a Milky Way 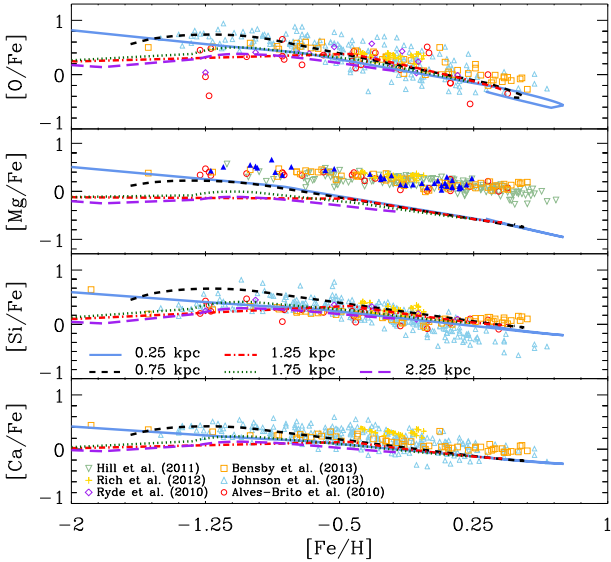sized galaxy. In this work we have adopted the Hernquist mass model (Hernquist 1990) for the GB in order to constraint the scenario that formed the GB:

$$M(r) = M_b \frac{r^2}{(r + a_b)^2}, \tag{1}$$

where $M_b$ is the GB mass, adopted to be $1.85 \times 10^{10} M_\odot$ (following Cavichia et al. et al. 2014) and the characteristic scalelength $a_b = r_{eff}(1 + \sqrt{2})^{-1} = 0.124$ kpc using $r_{eff} = 300$ pc

**Figure 2.** Comparison between the predictions of our model at different radial regions and the literature data for [α/Fe] where α stands for O, Mg, Si, and Ca, vs. [Fe/H]. The observational data for the bulge are labeled in the last panel (from top to bottom). The line codes of the models are as labeled in the third panel (from top to bottom). The observational data for the bulge are open circles from Alves-Brito et al. (2010), open squares from Bensby et al. (2013), open upside triangles from Johnson et al. (2013), open upside-down triangles from Hill et al. (2011), open stars from Rich et al. (2012), and open diamonds from Ryde et al. (2010).

(bulge half-light radius) from Wyse & Gilmore (1993). We divided the GB in five concentric regions, being the innermost a sphere of 0.25 kpc radius. The subsequent regions are spherical shells with external radii 0.75, 1.25, 1.75 and 2.25 kpc, each one 0.5 kpc wide. The Hernquist mass distribution is obtained allowing gas infalling first in the innermost spherical region and, when the mass distribution in that region resembles that from the Hernquist profile at the same radius, the infall ceases at this spherical region and begins at the following spherical shell. The total collapse-time scale to form the GB is 2 Gyr. The resulting GB metallicity distribution function (MDF) for each spherical region is shown in Fig. 1, represented by the [Fe/H] histograms. Double peak histograms are observed for each region, with exception of the outermost one, suggesting a GB composed by two populations with different mean metallicities. Probably in the outermost spherical shell there is an overlap between the disc and bulge population and the two component population is not observed. Nonetheless, it is evident in this figure the differences in the MDFs for each region. In the innermost one the fraction of the metal poor population is higher than the metal rich one. However, as moving further out to the other spherical shells, the fraction of metal poor stars decreases and the one from metal rich population increases. In spite of that, the positions of the peaks do not change considerably, considering the shells 0.75, 1.25 and 1.75 kpc. This results are in agreement with the most recent observations from Zoccali et al. (2017).

In Fig.2 it is shown [α/Fe] versus [Fe/H], where α stands for the α-elements: O, Mg, Si and Ca. Overall, our model is able to reproduce the observational data regarding the [O/Fe], [Si/Fe] and [Ca/Fe] abundance ratios. The [Ca/Fe] abundance ratio of Bensby et al. (2013) and Rich et al. (2012) are higher than the results of the model. In our case, we adopted the yields of O and Mg for high mass stars from Woosley & Weaver (1995) and it

is known that these yields needed to be increased in order to reproduce the most recent data of the bulge (Cavichia et al. et al. 2014 and Mollá et al. et al. 2015). Interesting, the model predicts different [α/Fe] ratios for each spherical region, the ratio being higher at the innermost regions (0.25 and 0.75 kpc) and lower at the outermost regions, especially at low [Fe/H] abundances. Higher [α/Fe] ratios at low [Fe/H] indicate a fast enrichment by massive stars which explode as type II supernovae. On the other hand, at higher metallicities ([Fe/H]> −0.5 dex) the differences in [α/Fe] ratios of the models are less important, probably because at these metallicities the type Ia supernovae have enriched the interstellar medium.

## 3. Discussion

The results of Fig. 2 suggest that the spread in [α/Fe] ratios, as shown by the observational data at lower metallicities, may be the result of mixing stars from different radial locations within the GB. Since the differences are in the range of ∼ 0.30 dex, it will be very difficult to detect this trend given the level of the uncertainties of the present observations. To confirm this possible gradient of [α/Fe] in the GB predicted by our models, more data with higher precision is needed, mainly for lower metallicities and galactocentric distances.

## References

Alves-Brito, A., Meléndez, J., Asplund, M., Ramírez, I., & Yong, D. 2010, A&A, 513, A35

Bensby, T., Yee, J. C., Feltzing, S., et al. 2013, A&A, 549, A147

Cavichia, O., Mollá, M., Costa, R. D. D., & Maciel, W. J. 2014, MNRAS, 437, 3688

Hernquist, L. 1990, ApJ, 356, 359

Hill, V., Lecureur, A., Gómez, A., et al. 2011, A&A, 534, A80

Johnson, C. I., Rich, R. M., Kobayashi, C., et al. 2013, ApJ, 765, 157

Mollá, M., & Díaz, A. I. 2005, MNRAS, 358, 521

Mollá, M., Cavichia, O., Gavilán, M., & Gibson, B. K. 2015, MNRAS, 451, 3693

Mollá, M., Díaz, Á. I., Gibson, B. K., Cavichia, O., & López-Sánchez, Á.-R. 2016, MNRAS, 462, 1329

Rich, R. M., Origlia, L., & Valenti, E. 2012, ApJ, 746, 59

Rojas-Arriagada, A., Recio-Blanco, A., Hill, V., et al. 2014, A&A, 569, A103

Ryde, N., Gustafsson, B., Edvardsson, B., et al. 2010, A&A, 509, A20

Woosley, S. E., & Weaver, T. A. 1995, ApJS, 101, 181

Wyse, R. F. G., & Gilmore, G. 1993, Galaxy Evolution. The Milky Way Perspective, 49, 209

Zoccali, M., Hill, V., Lecureur, A., et al. 2008, A&A, 486, 177

Zoccali, M., Vasquez, S., Gonzalez, O. A., et al. 2017, A&A, 599, A12